

# Generalized $\mathbb{Z}_p$ toric codes as qudit low-density parity-check codes

Zijian Liang<sup>1</sup> and Yu-An Chen<sup>1,\*</sup>

<sup>1</sup>*International Center for Quantum Materials, School of Physics, Peking University, Beijing 100871, China*

(Dated: February 24, 2026)

We study two-dimensional translation-invariant CSS stabilizer codes over prime-dimensional qudits on the square lattice under twisted boundary conditions, generalizing the Kitaev  $\mathbb{Z}_p$  toric code by augmenting each stabilizer with two additional qudits. Using the Laurent-polynomial formalism, we adapt the Gröbner basis to compute the logical dimension  $k$  efficiently, without explicitly constructing large parity-check matrices. We then perform a systematic search over various stabilizer realizations and lattice geometries for  $p \in \{3, 5, 7, 11\}$ , identifying qudit low-density parity-check codes with the optimal finite-size performance. Representative examples include  $[[242, 10, 22]]_3$  and  $[[120, 6, 20]]_{11}$ , both achieving  $kd^2/n = 20$ . Across the searched regime, the best observed  $kd^2$  at fixed  $n$  increases with  $p$ , with an empirical relation  $kd^2 = 0.0541 n^2 \ln p + 3.84 n$ , compatible with a Bravyi–Poulin–Terhal-type tradeoff when the interaction range grows with system size.

**Introduction.**— Fault-tolerant quantum computation requires active protection against noise, and quantum error-correcting codes are essential to achieve this goal [1–5]. Topological stabilizer codes, such as toric codes, are promising because they use local parity checks to achieve high thresholds on two-dimensional architectures [6–18]. Recent developments on bivariate bicycle (BB) codes show that two-dimensional translation-invariant CSS codes with weight-6 checks can outperform the standard toric code on relatively small tori, with performance improved by nearly an order of magnitude [19–32]. Most of the existing literature, however, focuses on qubit codes, even though several experimental platforms naturally realize higher-level systems such as qutrits or more general qudits [33–41]. This motivates the question of how to design and analyze efficient quantum low-density parity-check (LDPC) codes directly in the qudit setting [42].

At an abstract level, two-dimensional translation-invariant Pauli stabilizer codes over prime-dimensional qudits that satisfy the topological order (TO) condition are known to be locally equivalent to stacks of  $\mathbb{Z}_p$  toric codes and trivial product states [43–51]. The language of topological order and topological quantum field theory (TQFT) [52–88], such as anyon types, fusion and braiding, ground-state degeneracy, and Wilson-line operators, can therefore be imported directly into the qudit stabilizer setting. From this perspective, a  $\mathbb{Z}_p$  qudit stabilizer code can be viewed as a discrete  $\mathbb{Z}_p$  topological gauge theory equipped with a built-in notion of topological excitations and their syndromes.

In parallel, an algebraic viewpoint based on Laurent polynomial rings provides a powerful framework for analyzing translation-invariant stabilizer codes [31, 46, 47, 89]. By representing Pauli operators as modules over the polynomial ring  $\mathcal{R} = \mathbb{Z}_p[x^{\pm 1}, y^{\pm 1}]$ , one encodes locality and translation invariance into polynomial data and extracts the associated anyon content via ring-theoretic methods. Gröbner-basis techniques then enable efficient

computation of the ground-state degeneracy and logical operators on twisted tori, without constructing large parity-check matrices. In this work, we adapt this machinery to prime-dimensional qudits, focusing on generalized  $\mathbb{Z}_p$  toric codes in which the standard  $X$ -star and  $Z$ -plaquette stabilizers are augmented by two additional qudits, yielding weight-6 checks. We then systematically search for low-overhead qudit LDPC codes at system sizes of a few hundred qudits.

**Summary of results.**— We study two-dimensional translation-invariant CSS codes over  $\mathbb{Z}_p$  qudits with  $p \in \{3, 5, 7, 11\}$ , specified by a pair of Laurent polynomials  $f(x, y), g(x, y) \in \mathcal{R}$ . This polynomial data determines the stabilizers of generalized  $\mathbb{Z}_p$  toric codes on twisted tori. We systematically enumerate local stabilizer realizations together with twisted boundary conditions, and compute the corresponding code parameters  $[[n, k, d]]_p$ , where  $n$  is the number of physical qudits,  $k$  is the number of logical qudits, and  $d$  is the code distance. For  $p = 3$  we search system sizes up to  $n \leq 250$ , while for  $p \in \{5, 7, 11\}$  we search up to  $n \leq 150$ . The resulting high-performing qudit LDPC codes and their  $[[n, k, d]]_p$  parameters are summarized in Tables I–IV.

We explicitly present these  $[[n, k, d]]_p$  codes via their stabilizers (Fig. 1(a)) and the twisted torus (Fig. 1(b)). For fixed parameters  $[[n, k, d]]_p$ , there are typically many choices of stabilizer polynomials and lattice vectors; in the tables, we highlight realizations with the most local stabilizers, which are most promising for implementation on qudit hardware. Representative examples include

$[[52, 8, 7]]_3, [[78, 6, 11]]_3, [[156, 10, 15]]_3, [[242, 10, 22]]_3,$   
 $[[30, 4, 7]]_5, [[40, 4, 9]]_5, [[78, 10, 9]]_5, [[120, 6, 17]]_5,$   
 $[[28, 4, 7]]_7, [[96, 6, 15]]_7, [[98, 10, 12]]_7, [[144, 6, 21]]_7,$   
 $[[40, 4, 10]]_{11}, [[100, 6, 17]]_{11}, [[120, 6, 20]]_{11}, [[144, 6, 23]]_{11}.$

In particular, the codes  $[[242, 10, 22]]_3$  and  $[[120, 6, 20]]_{11}$  both attain  $kd^2/n = 20$ ; their stabilizers and twisted tori are shown in Fig. 2. Moreover, within the searched regime the best observed  $kd^2$  at fixed  $n$  increases with  $p$ , shown as Fig. 3, and the fit in Fig. 4 yields the empirical relation  $kd^2 = 0.0541 n^2 \ln p + 3.84 n$ .

\* E-mail: [yuanchen@pku.edu.cn](mailto:yuanchen@pku.edu.cn)

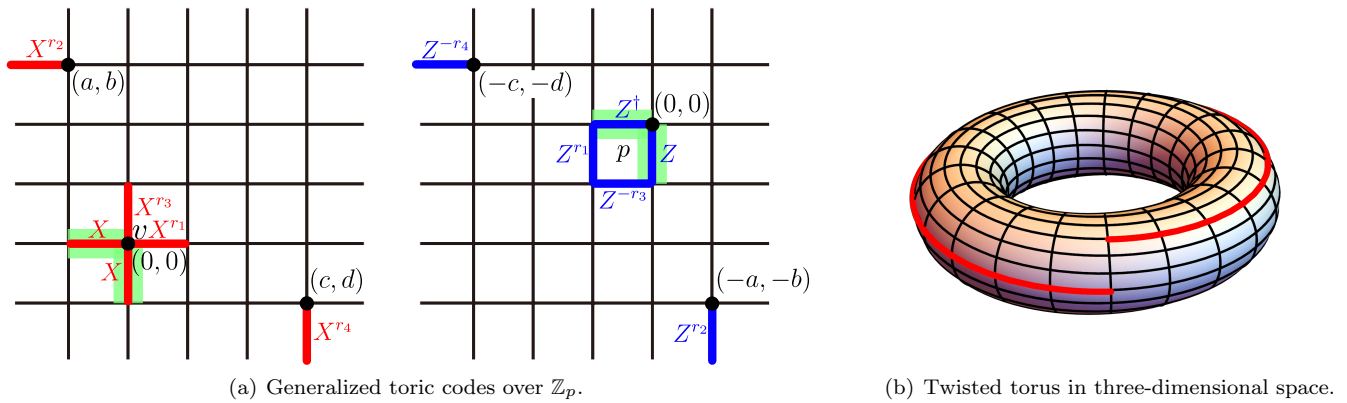


FIG. 1. (a) The  $A_v$  and  $B_p$  stabilizers of the generalized  $\mathbb{Z}_p$  toric codes, parameterized by the Laurent polynomials  $f(x, y) = 1 + r_1x + r_2x^a y^b$  and  $g(x, y) = 1 + r_3y + r_4x^c y^d$  in Eq. (5), with  $r_1, r_2, r_3, r_4 \in \mathbb{Z}_p \setminus \{0\}$  and  $a, b, c, d \in \mathbb{Z}$ . The green-shaded edges denote the unit cell at the origin used to generate the Pauli module over the Laurent polynomial ring [46]. For the same pair  $(f, g)$ , different choices of twisted boundary conditions can realize distinct quantum LDPC codes. (b) Adapted from Ref. [90]. A twisted torus embedded in three-dimensional space. The twist is applied along the longitudinal cycle by an angle that is a fraction of  $2\pi$ , as indicated by the red curve tracing a noncontractible cycle. The twisted torus is specified by two vectors  $\vec{a}_1 = (0, \alpha)$  and  $\vec{a}_2 = (\beta, \gamma)$ , i.e., lattice sites are identified by  $\vec{v} \sim \vec{v} + \vec{a}_1 \sim \vec{v} + \vec{a}_2$  for all  $\vec{v}$ .

**Review of ring-theoretical approach for bivariate bicycle codes.**— In this section, we review the algebraic framework for analyzing translation-invariant quantum codes on lattices [47]. We follow the notation of Ref. [90] and extend its Gröbner-basis analysis to  $\mathbb{Z}_p$  qudits. We begin by recalling the standard  $p \times p$  (generalized) Pauli operators for a  $\mathbb{Z}_p$  qudit:

$$X = \sum_{j \in \mathbb{Z}_p} |j+1\rangle\langle j|, \quad Z = \sum_{j \in \mathbb{Z}_p} \omega^j |j\rangle\langle j|. \quad (1)$$

where  $\omega$  is defined as  $\omega := \exp(\frac{2\pi i}{d})$ . More explicitly,

$$X = \begin{bmatrix} 0 & 0 & \cdots & 0 & 1 \\ 1 & 0 & \cdots & 0 & 0 \\ 0 & 1 & \cdots & 0 & 0 \\ \vdots & \vdots & \ddots & \vdots & \vdots \\ 0 & 0 & \cdots & 1 & 0 \end{bmatrix}, \quad Z = \begin{bmatrix} 1 & 0 & 0 & \cdots & 0 \\ 0 & \omega & 0 & \cdots & 0 \\ 0 & 0 & \omega^2 & \cdots & 0 \\ \vdots & \vdots & \vdots & \ddots & \vdots \\ 0 & 0 & 0 & \cdots & \omega^{d-1} \end{bmatrix}, \quad (2)$$

and  $X$  and  $Z$  satisfy the commutation relation

$$ZX = \omega XZ. \quad (3)$$

For simplicity, we focus on the square lattice with one  $\mathbb{Z}_p$  qudit living at each edge. We briefly review the polynomial representation of Pauli operators [46]. A unit cell contains two vertices,  $e_1$  and  $e_2$ , whose Pauli operators are represented by four-dimensional vectors:

$$\mathcal{X}_{e_1} = \begin{bmatrix} 1 \\ 0 \\ 0 \\ 0 \end{bmatrix}, \quad \mathcal{Z}_{e_1} = \begin{bmatrix} 0 \\ 0 \\ 1 \\ 0 \end{bmatrix}, \quad \mathcal{X}_{e_2} = \begin{bmatrix} 0 \\ 1 \\ 0 \\ 0 \end{bmatrix}, \quad \mathcal{Z}_{e_2} = \begin{bmatrix} 0 \\ 0 \\ 0 \\ 1 \end{bmatrix}. \quad (4)$$

A translation by  $(n, m) \in \mathbb{Z}^2$  is implemented by multiplying the corresponding vector by the monomial  $x^n y^m$ .

More generally, any Pauli operator (modulo an overall phase) is represented by a vector in  $\mathcal{R}^4$ , where  $\mathcal{R} = \mathbb{Z}_p[x^{\pm 1}, y^{\pm 1}]$ . Vector addition corresponds to operator multiplication, while multiplication by elements of  $\mathcal{R}$  encodes lattice translations and  $\mathbb{Z}_p$  exponents. Thus, the Pauli group modulo phase is naturally identified with an  $\mathcal{R}$ -module.

A translation-invariant CSS code is specified by a pair of Laurent polynomials  $f, g \in \mathcal{R}$ :

$$A_v = \begin{bmatrix} f(x, y) \\ g(x, y) \\ 0 \\ 0 \end{bmatrix}, \quad B_p = \begin{bmatrix} 0 \\ 0 \\ \overline{-g(x, y)} \\ \overline{f(x, y)} \end{bmatrix}, \quad (5)$$

where  $\overline{(\cdot)}$  denotes the antipode map  $x^n y^m \mapsto x^{-n} y^{-m}$ . The stabilizer group is generated by all lattice translates of  $A_v$  and  $B_p$ . As a simple example, the Kitaev toric code [6] corresponds to  $f(x, y) = 1 - x$  and  $g(x, y) = 1 - y$ .

The topological order condition is satisfied when  $f(x, y)$  and  $g(x, y)$  are coprime [31], which ensures that any local operator commuting with all stabilizers is itself a stabilizer. Moreover, the maximal number of logical qudits on a torus equals the number of independent anyon generators in the underlying topological order [92–94]. It can be computed from the codimension of the ideal generated by  $f$  and  $g$ :

$$k_{\max} = 2 \dim \left( \frac{\mathbb{Z}_p[x^{\pm 1}, y^{\pm 1}]}{\langle f, g \rangle} \right). \quad (6)$$

For twisted boundary conditions specified by  $\vec{a}_1 = (0, \alpha)$  and  $\vec{a}_2 = (\beta, \gamma)$ , the resulting code has logical dimension [90]

$$k = 2 \dim \left( \frac{\mathbb{Z}_p[x^{\pm 1}, y^{\pm 1}]}{\langle f(x, y), g(x, y), y^\alpha - 1, x^\beta y^\gamma - 1 \rangle} \right). \quad (7)$$

$[[n, k, d]]_3$	$f(x, y)$	$g(x, y)$	$\vec{a}_1$	$\vec{a}_2$	$\frac{kd^2}{n}$
$[[16, 4, 4]]_3$	$1 + x + y$	$1 + y - x^{-1}y$	(0, 4)	(2, 1)	4
$[[26, 6, 5]]_3$	$1 + x + x^{-1}y$	$1 - y - x^{-1}$	(0, 13)	(1, 5)	5.77
$[[42, 4, 8]]_3$	$1 + x + x^{-2}y^{-1}$	$1 + y + x$	(0, 3)	(7, 1)	6.10
$[[48, 4, 9]]_3$	$1 - x + xy^2$	$1 - y + x^2$	(0, 8)	(3, 3)	6.75
$[[52, 8, 7]]_3$	$1 + x + x^{-1}y^{-2}$	$1 + y + xy^{-1}$	(0, 13)	(2, 5)	7.54
$[[64, 4, 11]]_3$	$1 + x + x^{-1}y^{-2}$	$1 + y - x^{-1}y^2$	(0, 16)	(2, 7)	7.56
$[[72, 4, 12]]_3$	$1 - x + y^2$	$1 - y + x^2$	(0, 12)	(3, 3)	8
$[[78, 6, 11]]_3$	$1 + x + x^{-1}y^2$	$1 - y + x^{-2}y^{-1}$	(0, 13)	(3, 4)	9.31
$[[104, 6, 14]]_3$	$1 - x + xy^{-3}$	$1 - y + x^{-2}y^2$	(0, 26)	(2, -9)	11.31
$[[130, 6, 16]]_3$	$1 + x + x^2y^3$	$1 + y - x^{-2}y^2$	(0, 13)	(5, 3)	11.82
$[[144, 6, 17]]_3$	$1 + x + x^2y^2$	$1 + y + xy^{-3}$	(0, 36)	(2, 15)	12.04
$[[156, 10, 15]]_3$	$1 + x + x^{-1}y^2$	$1 + y + x^{-3}y^2$	(0, 26)	(3, 4)	14.42
$[[160, 12, 14]]_3$	$1 - x - x^{-2}y^2$	$1 - y - x^{-3}y^{-2}$	(0, 40)	(2, 7)	14.7
$[[192, 8, 19]]_3$	$1 + x + x^2y^{-2}$	$1 + y + x^3y$	(0, 16)	(6, 7)	15.04
$[[208, 8, 20]]_3$	$1 - x + xy^{-3}$	$1 - y + x^{-2}y^2$	(0, 26)	(4, 8)	15.38
$[[224, 6, 24]]_3$	$1 + x + x^2y^2$	$1 + y + xy^{-3}$	(0, 56)	(2, 15)	15.43
$[[234, 6, 25]]_3$	$1 + x - x^2y^{-6}$	$1 + y + x^2y^3$	(0, 13)	(9, 2)	16.03
$[[240, 8, 22]]_3$	$1 + x + xy^{-5}$	$1 + y + x^5$	(0, 60)	(2, 13)	16.13
$[[242, 10, 22]]_3$	$1 - x + x^3y^{-3}$	$1 - y + x^{-4}$	(0, 11)	(11, 4)	20

TABLE I.  $\mathbb{Z}_3$  qutrit LDPC codes with  $n \leq 250$ . The Laurent polynomials  $f(x, y)$  and  $g(x, y)$  specify the translation-invariant stabilizers, while the vectors  $\vec{a}_1$  and  $\vec{a}_2$  define the twisted boundary conditions of the torus (see Fig. 1). We list  $[[n, k, d]]_3$  such that  $kd^2/n$  for each entry in the table exceeds that of all instances with smaller  $n$ . We emphasize that the code distances are obtained using the probabilistic algorithm of Ref. [91]; accordingly, the reported values of  $d$  are upper bounds on the exact distance. For each code, we sample 5,000–10,000 information sets and repeat the procedure 1,000 times to assess consistency, yielding upper bounds that we believe are tight in practice.

$[[n, k, d]]_5$	$f(x, y)$	$g(x, y)$	$\vec{a}_1$	$\vec{a}_2$	$\frac{kd^2}{n}$
$[[16, 4, 4]]_5$	$1 + x + 3y$	$1 + 3y + x^{-1}y$	(0, 4)	(2, 1)	4.00
$[[20, 4, 5]]_5$	$1 + 2x + 4x^{-1}y$	$1 + 3y + 4x$	(0, 5)	(2, 1)	5.00
$[[24, 4, 6]]_5$	$1 + 2x + 2xy$	$1 + 3y + x^{-1}y$	(0, 4)	(3, 2)	6.00
$[[30, 4, 7]]_5$	$1 + x + 3x^2y^{-1}$	$1 + 2y + 2x^2y$	(0, 15)	(1, 6)	6.53
$[[40, 4, 9]]_5$	$1 + x + 3x^2y^{-1}$	$1 + 3y + x^2y$	(0, 4)	(5, 1)	8.10
$[[48, 4, 10]]_5$	$1 + x + 4x^{-1}y^{-1}$	$1 + y + 2xy^{-1}$	(0, 6)	(4, 3)	8.33
$[[56, 4, 11]]_5$	$1 + 2x + 2x^{-2}$	$1 + 2y + 2x^{-1}y^{-1}$	(0, 4)	(7, 1)	8.64
$[[62, 6, 10]]_5$	$1 + 2x + 4y^2$	$1 + 4y + 3x^2y$	(0, 31)	(1, 7)	9.68
$[[78, 10, 9]]_5$	$1 + 2x + 2x^2y^2$	$1 + 3y + x^{-3}$	(0, 39)	(1, 5)	10.38
$[[80, 6, 12]]_5$	$1 + x + 3x^{-2}$	$1 + 3y + xy^{-2}$	(0, 10)	(4, 4)	10.80
$[[90, 4, 16]]_5$	$1 + x + x^{-2}y$	$1 + y + x^{-1}y^3$	(0, 9)	(5, 1)	11.38
$[[96, 6, 14]]_5$	$1 + 2x + 2x^2y$	$1 + 2y + 3x^{-1}y^2$	(0, 16)	(3, 6)	12.25
$[[114, 4, 19]]_5$	$1 + x + x^{-1}y^{-2}$	$1 + y + 3x^3$	(0, 19)	(3, 7)	12.67
$[[120, 6, 17]]_5$	$1 + x + 3y^3$	$1 + 2y + 2xy^3$	(0, 30)	(2, 13)	14.45
$[[124, 6, 18]]_5$	$1 + x + 3x^3y^{-2}$	$1 + 3y + 4x^3y$	(0, 31)	(2, 12)	15.68
$[[144, 6, 20]]_5$	$1 + x + 3x^{-2}y$	$1 + y + 3x^2y^3$	(0, 9)	(8, 1)	16.67

TABLE II.  $\mathbb{Z}_5$  qudit LDPC codes with  $n \leq 150$ . Similar to Table I.

The derivations of Eqs. (6) and (7) for  $\mathbb{Z}_p$  qudits follow directly from the corresponding proofs for the  $\mathbb{Z}_2$  case established previously in Refs. [90, 95]. The right-hand side of Eq. (7) can be evaluated efficiently using a Gröbner basis computed via Buchberger’s algorithm [96].

**Search for bivariate bicycle codes over  $\mathbb{Z}_p$ .**— We

$[[n, k, d]]_7$	$f(x, y)$	$g(x, y)$	$\vec{a}_1$	$\vec{a}_2$	$\frac{kd^2}{n}$
$[[12, 4, 3]]_7$	$1 + 2x + 5y$	$1 + 2y + 2x^{-1}$	(0, 2)	(3, 0)	3.00
$[[14, 4, 4]]_7$	$1 + 2x + 4xy$	$1 + 4y + 2xy$	(0, 7)	(1, 3)	4.57
$[[24, 4, 6]]_7$	$1 + 2x + 5y$	$1 + 2y + 2x^{-1}$	(0, 4)	(3, 2)	6.00
$[[28, 4, 7]]_7$	$1 + 5x + x^{-1}y^{-1}$	$1 + 5y + x$	(0, 7)	(2, 3)	7.00
$[[32, 4, 8]]_7$	$1 + x + 2x^2y$	$1 + 2y + 3x^{-1}y^2$	(0, 4)	(4, 1)	8.00
$[[48, 4, 10]]_7$	$1 + x + 5x^2y$	$1 + 3y + 3x^{-1}y^2$	(0, 8)	(3, 3)	8.33
$[[56, 4, 12]]_7$	$1 + x + 5xy$	$1 + 2y + 4xy^{-2}$	(0, 7)	(4, 1)	10.29
$[[64, 4, 13]]_7$	$1 + 2x + 2x^{-1}y^{-2}$	$1 + 4y + 5xy^{-1}$	(0, 8)	(4, 1)	10.56
$[[70, 4, 14]]_7$	$1 + x + 5xy^{-2}$	$1 + 4y + 2x^{-2}y^{-1}$	(0, 7)	(5, 1)	11.20
$[[76, 6, 12]]_7$	$1 + x + x^{-1}y^2$	$1 + 2y + 4x^{-1}y^{-1}$	(0, 19)	(2, 7)	11.37
$[[84, 4, 16]]_7$	$1 + x + x^{-1}y^{-2}$	$1 + y + 3x^2y^{-2}$	(0, 14)	(3, 5)	12.19
$[[96, 6, 15]]_7$	$1 + x + y^2$	$1 + 4y + 5x^{-2}$	(0, 16)	(3, 5)	14.06
$[[98, 10, 12]]_7$	$1 + 2x + 4x^{-1}y^2$	$1 + 4y + 2x^{-2}y^{-1}$	(0, 7)	(7, 0)	14.69
$[[126, 6, 18]]_7$	$1 + x + x^2y^2$	$1 + 3y + 3x^3$	(0, 21)	(3, 15)	15.43
$[[128, 6, 19]]_7$	$1 + x + 5x^3y^{-2}$	$1 + 2y + 4xy^{-4}$	(0, 16)	(4, 7)	16.92
$[[144, 6, 21]]_7$	$1 + x + 3x^2y^{-2}$	$1 + y + 5x^{-1}y^{-2}$	(0, 12)	(6, 3)	18.38

TABLE III.  $\mathbb{Z}_7$  qudit LDPC codes with  $n \leq 150$ . Similar to Table I.

$[[n, k, d]]_{11}$	$f(x, y)$	$g(x, y)$	$\vec{a}_1$	$\vec{a}_2$	$\frac{kd^2}{n}$
$[[16, 4, 4]]_{11}$	$1 + 7x + 4xy$	$1 + 10y + 3x^{-1}y^2$	(0, 4)	(2, 1)	4.00
$[[20, 4, 5]]_{11}$	$1 + x + 2xy$	$1 + 7y + 10xy^{-1}$	(0, 5)	(2, 1)	5.00
$[[22, 4, 6]]_{11}$	$1 + 5x + 5x^{-1}$	$1 + 8y + 2xy^{-1}$	(0, 11)	(1, 3)	6.55
$[[32, 4, 8]]_{11}$	$1 + 3x + 10y^3$	$1 + 10y + 3x^{-1}y^2$	(0, 8)	(2, 1)	8.00
$[[40, 4, 10]]_{11}$	$1 + x + 10x^{-1}y^{-1}$	$1 + 7y + 10xy^{-1}$	(0, 10)	(2, 4)	10.00
$[[48, 4, 11]]_{11}$	$1 + 3x + x^{-1}y$	$1 + 6y + x^{-1}y^{-1}$	(0, 6)	(4, 1)	10.08
$[[60, 4, 13]]_{11}$	$1 + x + 9x^2y^2$	$1 + 5y + 5xy^{-1}$	(0, 5)	(6, 2)	11.27
$[[66, 4, 14]]_{11}$	$1 + 5x + 5y^2$	$1 + 8y + 2x^2$	(0, 11)	(3, 6)	11.88
$[[72, 4, 15]]_{11}$	$1 + 2x + 9x^{-1}y^{-2}$	$1 + 5y + 2x^{-2}y^2$	(0, 12)	(3, 5)	12.50
$[[80, 6, 14]]_{11}$	$1 + x + 2x^{-2}y^{-1}$	$1 + 8y + 7xy^{-2}$	(0, 10)	(4, 4)	14.70
$[[96, 6, 16]]_{11}$	$1 + 2x + 8xy^{-3}$	$1 + 3y + 7x^{-2}y^2$	(0, 16)	(3, 3)	16.00
$[[100, 6, 17]]_{11}$	$1 + x + x^{-2}y^{-1}$	$1 + 5y + 10x^2y^{-1}$	(0, 10)	(5, 5)	17.34
$[[120, 6, 20]]_{11}$	$1 + x + 2x^{-2}y^3$	$1 + y + 4x^{-1}y^{-4}$	(0, 10)	(6, 2)	20.00
$[[144, 6, 23]]_{11}$	$1 + 2x + 8x^{-2}y^2$	$1 + 2y + 8x^{-2}y^{-3}$	(0, 8)	(9, 1)	22.04

TABLE IV.  $\mathbb{Z}_{11}$  qudit LDPC codes with  $n \leq 150$ . Similar to Table I.

introduce the *generalized toric code* over  $\mathbb{Z}_p$ , a particular subclass of bivariate bicycle (BB) codes, defined by

$$\begin{aligned} f(x, y) &= 1 + r_1x + r_2x^a y^b, \\ g(x, y) &= 1 + r_3y + r_4x^c y^d, \end{aligned} \quad (8)$$

with  $r_i \in \mathbb{Z}_p \setminus \{0\}$  and  $a, b, c, d \in \mathbb{Z}$ , as illustrated in Fig. 1(a).

We systematically search for high-performing weight-6 BB codes of the form (8) over  $\mathbb{Z}_p$  qudits with twisted-periodic boundary conditions. For each even  $n$ , we enumerate all factorizations  $n = 2\alpha\beta$  and define a twisted torus by the basis vectors  $\vec{a}_1 = (0, \alpha)$  and  $\vec{a}_2 = (\beta, \gamma)$  with  $0 \leq \gamma < \beta$ . We then enumerate all polynomials of the form (8) whose exponent pairs  $(a, b)$  and  $(c, d)$  lie within the fundamental parallelogram spanned by  $\vec{a}_1$  and  $\vec{a}_2$ . For each candidate, we compute the corresponding logical dimension  $k$  using Eq. (7). The computational cost of evaluating  $k$  in Eq. (7) is essentially independent of system size: the boundary relations  $y^\alpha - 1$  and  $x^\beta y^\gamma - 1$  are reduced modulo the ideal  $\langle f, g \rangle$ , and only the

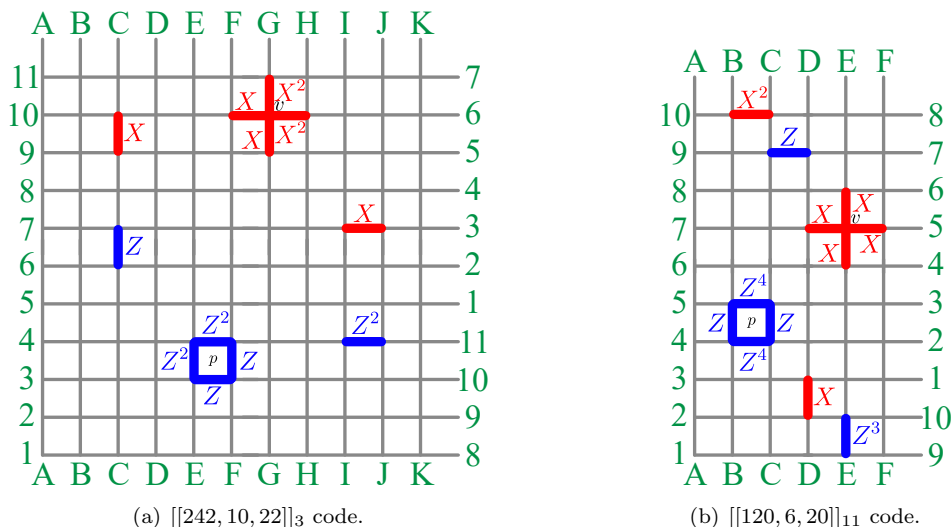
(a)  $[[242, 10, 22]]_3$  code.(b)  $[[120, 6, 20]]_{11}$  code.

FIG. 2. Representative stabilizer realizations on twisted tori. (a)  $X$ - and  $Z$ -stabilizers of the  $[[242, 10, 22]]_3$  code with  $f = 1 - x + x^3 y^{-3}$  and  $g = 1 - y + x^{-4}$ , defined with twisted boundary vectors  $\vec{a}_1 = (0, 11)$  and  $\vec{a}_2 = (11, 4)$ . (b)  $X$ - and  $Z$ -stabilizers of the  $[[120, 6, 20]]_{11}$  code with  $f = 1 + x + 2x^{-2}y^3$  and  $g = 1 + y + 4x^{-1}y^{-4}$ , defined with  $\vec{a}_1 = (0, 10)$  and  $\vec{a}_2 = (6, 2)$ . All other stabilizers are obtained by translations. In each panel, vertices with the same letter (top/bottom) or the same number (left/right) are identified, yielding a twisted torus.

resulting remainders enter the Gröbner-basis dimension calculation. For instances with  $k > 0$ , we then compute the code distance  $d$  using the probabilistic algorithm [91], thereby obtaining the full  $[[n, k, d]]_p$  parameters.

The results for qudit LDPC codes over  $\mathbb{Z}_p$  with  $p = 3, 5, 7, 11$  are summarized in Tables I–IV, covering  $p = 3$  with  $n \leq 250$  and  $p = 5, 7, 11$  with  $n \leq 150$ . When multiple codes achieve the same optimal  $kd^2/n$ , we select the one with the most local stabilizers as the representative example.

By comparing the  $\mathbb{Z}_2$  results [90] summarized in Appendix A with our data for  $\mathbb{Z}_3, \mathbb{Z}_5, \mathbb{Z}_7$ , and  $\mathbb{Z}_{11}$ , we obtain the plot in Fig. 3(a). The vertical axis shows the figure of merit  $kd^2/n$ , while the horizontal axis shows the minimum number of physical qudits  $n$  required to achieve a given value of  $kd^2/n$ .

For each fixed  $p$ , the dependence of  $kd^2/n$  on  $n$  is approximately linear over the fitted range, with coefficient of determination  $R^2 \approx 0.95\text{--}0.98$ . Moreover, at fixed  $n$  we observe that the best achievable  $kd^2/n$  increases with the qudit dimension  $p$ . For example, at comparable performance, the  $[[120, 6, 20]]_{11}$  code ( $kd^2/n = 20$ ) uses  $n = 120$  qudits, whereas the best  $\mathbb{Z}_2$  instance in our comparison,  $[[360, 12, 24]]_2$  ( $kd^2/n = 19.2$ ), requires  $n = 360$  qubits. Finally, the linear fits in Fig. 3(a) suggest that the fitted slope of  $kd^2/n$  versus  $n$  grows approximately as  $\ln p$ , as summarized in Fig. 3(b).

**Relation to the Bravyi–Poulin–Terhal Tradeoff.**— Motivated by the trend in  $kd^2/n$  across different primes  $p$  in Fig. 3, we replot the same data in Fig. 4 as  $kd^2/n$  versus  $(\ln p)n$  and perform a linear least-squares fit, obtaining

$$kd^2 = 0.0541 n^2 \ln p + 3.84 n, \quad (9)$$

for the explored primes  $p \in \{2, 3, 5, 7, 11\}$ . At first glance, the quadratic dependence on  $n$  may seem to contradict the Bravyi–Poulin–Terhal (BPT) bound [97, 98], which states that for geometrically local stabilizer codes in two dimensions

$$kd^2 = O(n), \quad (10)$$

where the implicit constant depends on the interaction range  $r$  and the on-site Hilbert-space dimension.

To make this dependence explicit, we follow the BPT argument. The lattice is partitioned into an array of  $R \times R$  blocks such that each block is correctable, and the block corners are covered by a region  $C$ . By the cleaning lemma, one may choose  $R = \Omega(d/r)$ . The proof in Ref. [98] then implies

$$k \leq S(C) \leq |C| = O\left(\frac{nr^2}{R^2}\right) = O\left(\frac{nr^4}{d^2}\right), \quad (11)$$

where  $S(C)$  denotes the entanglement entropy of region  $C$ . Here, we use the fact that each corner region has linear size  $O(r)$  (and hence area  $O(r^2)$ ), and that the number of blocks is  $n/R^2$ . It follows that

$$kd^2 = O(nr^4). \quad (12)$$

Superlinear behavior in  $n$  is therefore compatible with BPT whenever the interaction range  $r$  increases with system size. In our generalized toric constructions, the geometric diameter of the weight-6 stabilizers can grow with  $n$ , depending on the chosen exponents in  $f(x, y)$  and  $g(x, y)$ . This relaxes the BPT constraint and is consistent with the empirical relation (9).

**Discussion and future directions.**— We have developed a topological-order perspective on translation-invariant  $\mathbb{Z}_p$  stabilizer codes on twisted tori. In this

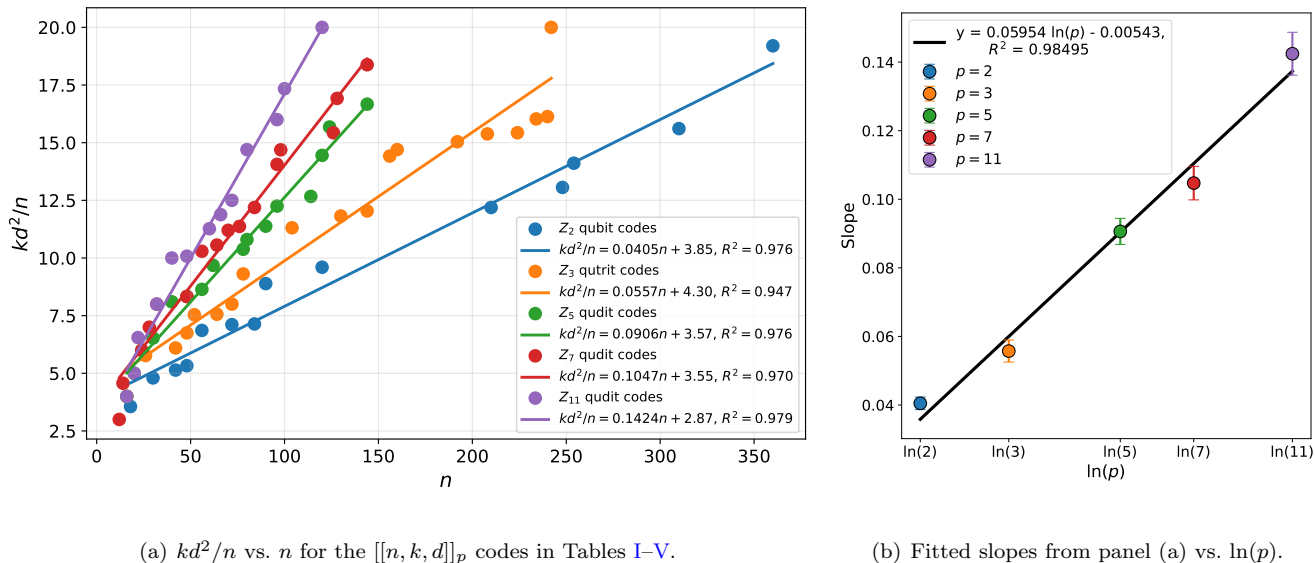


FIG. 3. Finite-size performance across qudit dimensions. (a)  $[[n, k, d]]_p$  LDPC codes from Tables I–V: the metric  $kd^2/n$  is plotted versus block length  $n$  for  $p \in \{2, 3, 5, 7, 11\}$ , together with linear fits for each  $p$ . (b) Slopes extracted from the fits in panel (a), plotted against  $\ln(p)$ , with error bars given by the standard errors from the linear fits in panel (a). Linear regression indicates an approximately linear dependence on  $\ln(p)$ .

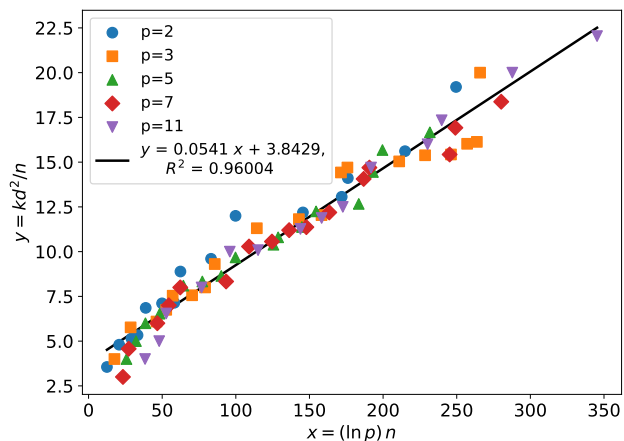


FIG. 4. Finite-size performance metric  $kd^2/n$  for all code instances listed in Tables I–V, plotted against  $(\ln p)n$  for the explored primes  $p \in \{2, 3, 5, 7, 11\}$ . The solid line is the least-squares linear fit  $kd^2/n = 0.0541(\ln p)n + 3.84$  with  $R^2 = 0.96$ .

framework, the logical dimension  $k$  is determined by the anyon algebra and computed as the dimension of the quotient ring  $\mathcal{R}/I$ , where  $I = \langle f(x, y), g(x, y) \rangle$  is the stabilizer ideal. This ring-theoretic approach naturally incorporates twisted boundary conditions and, together with Gröbner-basis techniques, enables efficient characterization and systematic searches for new qudit LDPC codes. The high-performing instances summarized in Tables I–IV provide a foundation for further theoretical and

hardware-oriented investigations.

Future work may extend the search to larger system sizes, where further improvements could emerge. Because the enumeration procedure is fully parallelizable, it can be scaled to  $n \leq 500$  or beyond using clusters or supercomputers, approaching the scale of current experimental platforms [99–104]. The primary computational bottleneck is distance estimation: for  $n$  of a few hundred and  $d > 25$ , existing probabilistic distance algorithms typically yield only upper bounds and may become unreliable. It will also be important to verify whether the empirical relation (9) persists at larger  $n$  and  $p$ , and to establish a theoretical understanding of the observed  $n^2 \ln p$  scaling.

Furthermore, allowing higher-weight stabilizers is another natural direction, as such constructions have led to improved  $[[n, k, d]]$  parameters in other quantum LDPC code families [22, 31, 105–116].

Finally, it will be important to assess the performance of these codes under circuit-level noise models [19]. In particular, syndrome-extraction circuits must be optimized for low depth, as the circuit-level distance is typically smaller than the code distance. Numerical simulations to estimate pseudo-thresholds, along with the development of efficient logical-gate implementations and hardware realizations, will be essential steps toward practical deployment.

**Acknowledgement.**— This work is supported by the National Natural Science Foundation of China (Grant No. 12474491) and the Fundamental Research Funds for the Central Universities, Peking University.

- 
- [1] Peter W. Shor, “Scheme for reducing decoherence in quantum computer memory,” *Phys. Rev. A* **52**, R2493–R2496 (1995).
- [2] A. M. Steane, “Error correcting codes in quantum theory,” *Phys. Rev. Lett.* **77**, 793–797 (1996).
- [3] Emanuel Knill and Raymond Laflamme, “Theory of quantum error-correcting codes,” *Phys. Rev. A* **55**, 900–911 (1997).
- [4] Daniel Gottesman, “Stabilizer codes and quantum error correction,” (1997), [arXiv:quant-ph/9705052](https://arxiv.org/abs/quant-ph/9705052) [quant-ph].
- [5] A. Yu. Kitaev, “Fault-tolerant quantum computation by anyons,” *Annals of Physics* **303**, 2–30 (2003).
- [6] Sergey B Bravyi and A Yu Kitaev, “Quantum codes on a lattice with boundary,” [arXiv preprint quant-ph/9811052](https://arxiv.org/abs/quant-ph/9811052) (1998).
- [7] Eric Dennis, Alexei Kitaev, Andrew Landahl, and John Preskill, “Topological quantum memory,” *Journal of Mathematical Physics* **43**, 4452–4505 (2002).
- [8] G. Semeghini, H. Levine, A. Keesling, S. Ebadi, T. T. Wang, D. Bluvstein, R. Verresen, H. Pichler, M. Kalinowski, R. Samajdar, A. Omran, S. Sachdev, A. Vishwanath, M. Greiner, V. Vuletić, and M. D. Lukin, “Probing topological spin liquids on a programmable quantum simulator,” *Science* **374**, 1242–1247 (2021).
- [9] Ruben Verresen, Mikhail D. Lukin, and Ashvin Vishwanath, “Prediction of toric code topological order from rydberg blockade,” *Phys. Rev. X* **11**, 031005 (2021).
- [10] Nikolas P. Breuckmann and Jens Niklas Eberhardt, “Quantum low-density parity-check codes,” *PRX Quantum* **2**, 040101 (2021).
- [11] Dolev Bluvstein, Harry Levine, Giulia Semeghini, Tout T. Wang, Sepehr Ebadi, Marcin Kalinowski, Alexander Keesling, Nishad Maskara, Hannes Pichler, Markus Greiner, Vladan Vuletić, and Mikhail D. Lukin, “A quantum processor based on coherent transport of entangled atom arrays,” *Nature* **604**, 451–456 (2022).
- [12] Google Quantum AI and Collaborators, “Suppressing quantum errors by scaling a surface code logical qubit,” *Nature* **614**, 676–681 (2023).
- [13] Google Quantum AI and Collaborators, “Non-abelian braiding of graph vertices in a superconducting processor,” *Nature* **618**, 264–269 (2023).
- [14] Google Quantum AI and Collaborators, “Quantum error correction below the surface code threshold,” *Nature* (2024), [10.1038/s41586-024-08449-y](https://doi.org/10.1038/s41586-024-08449-y).
- [15] Zijian Liang, Jens Niklas Eberhardt, and Yu-An Chen, “Planar quantum low-density parity-check codes with open boundaries,” *PRX Quantum* **6**, 040330 (2025).
- [16] Mohsin Iqbal, Nathanan Tantivasadakarn, Thomas M. Gatterman, Justin A. Gerber, Kevin Gilmore, Dan Gresh, Aaron Hankin, Nathan Hewitt, Chandler V. Horst, Mitchell Matheny, Tanner Mengle, Brian Neyenhuis, Ashvin Vishwanath, Michael Foss-Feig, Ruben Verresen, and Henrik Dreyer, “Topological order from measurements and feed-forward on a trapped ion quantum computer,” *Communications Physics* **7**, 205 (2024).
- [17] Mohsin Iqbal, Nathanan Tantivasadakarn, Ruben Verresen, Sara L. Campbell, Joan M. Dreiling, Caroline Figgatt, John P. Gaebler, Jacob Johansen, Michael Mills, Steven A. Moses, Juan M. Pino, Anthony Ransford, Mary Rowe, Peter Siegfried, Russell P. Stutz, Michael Foss-Feig, Ashvin Vishwanath, and Henrik Dreyer, “Non-abelian topological order and anyons on a trapped-ion processor,” *Nature* **626**, 505–511 (2024).
- [18] Iris Cong, Nishad Maskara, Minh C. Tran, Hannes Pichler, Giulia Semeghini, Susanne F. Yelin, Soonwon Choi, and Mikhail D. Lukin, “Enhancing detection of topological order by local error correction,” *Nature Communications* **15**, 1527 (2024).
- [19] Sergey Bravyi, Andrew W. Cross, Jay M. Gambetta, Dmitri Maslov, Patrick Rall, and Theodore J. Yoder, “High-threshold and low-overhead fault-tolerant quantum memory,” *Nature* **627**, 778–782 (2024).
- [20] Ming Wang and Frank Mueller, “Coprime bivariate bicycle codes and their properties,” [arXiv preprint arXiv:2408.10001](https://arxiv.org/abs/2408.10001) (2024).
- [21] Ming Wang and Frank Mueller, “Rate adjustable bivariate bicycle codes for quantum error correction,” in *2024 IEEE International Conference on Quantum Computing and Engineering (QCE)*, Vol. 02 (2024) pp. 412–413.
- [22] Ryan Tiew and Nikolas P Breuckmann, “Low-overhead entangling gates from generalised dehn twists,” [arXiv preprint arXiv:2411.03302](https://arxiv.org/abs/2411.03302) (2024).
- [23] Stasiu Wolanski and Ben Barber, “Ambiguity clustering: an accurate and efficient decoder for qldpc codes,” [arXiv preprint arXiv:2406.14527](https://arxiv.org/abs/2406.14527) (2024).
- [24] Anqi Gong, Sebastian Cammerer, and Joseph M Renes, “Toward low-latency iterative decoding of qldpc codes under circuit-level noise,” [arXiv preprint arXiv:2403.18901](https://arxiv.org/abs/2403.18901) (2024).
- [25] Arshpreet Singh Maan and Alexandru Paler, “Machine learning message-passing for the scalable decoding of qldpc codes,” [arXiv preprint arXiv:2408.07038](https://arxiv.org/abs/2408.07038) (2024).
- [26] Alexander Cowtan, “Ssip: automated surgery with quantum ldpc codes,” [arXiv preprint arXiv:2407.09423](https://arxiv.org/abs/2407.09423) (2024).
- [27] Mackenzie H Shaw and Barbara M Terhal, “Lowering connectivity requirements for bivariate bicycle codes using morphing circuits,” [arXiv preprint arXiv:2407.16336](https://arxiv.org/abs/2407.16336) (2024).
- [28] Andrew Cross, Zhiyang He, Patrick Rall, and Theodore Yoder, “Linear-size ancilla systems for logical measurements in qldpc codes,” [arXiv preprint arXiv:2407.18393](https://arxiv.org/abs/2407.18393) (2024).
- [29] Lukas Voss, Sim Jian Xian, Tobias Haug, and Kishor Bharti, “Multivariate bicycle codes,” [arXiv preprint arXiv:2406.19151](https://arxiv.org/abs/2406.19151) (2024).
- [30] Noah Berthusen, Dhruv Devulapalli, Eddie Schoute, Andrew M. Childs, Michael J. Gullans, Alexey V. Gorshkov, and Daniel Gottesman, “Toward a 2d local implementation of quantum low-density parity-check codes,” *PRX Quantum* **6**, 010306 (2025).
- [31] Jens Niklas Eberhardt and Vincent Steffan, “Logical operators and fold-transversal gates of bivariate bicycle codes,” [arXiv preprint arXiv:2407.03973](https://arxiv.org/abs/2407.03973) (2024).
- [32] Hsiang-Ku Lin, Xingrui Liu, Pak Kau Lim, and Leonid P Pryadko, “Single-shot and two-shot decoding with generalized bicycle codes,” [arXiv preprint arXiv:2502.19406](https://arxiv.org/abs/2502.19406) (2025).

- [33] Noah Goss, Alexis Morvan, Brian Marinelli, Bradley K. Mitchell, Long B. Nguyen, Ravi K. Naik, Larry Chen, Christian Jünger, John Mark Kreikebaum, David I. Santiago, Joel J. Wallman, and Irfan Siddiqi, “High-fidelity qutrit entangling gates for superconducting circuits,” *Nature Communications* **13** (2022), [10.1038/s41467-022-34851-z](https://doi.org/10.1038/s41467-022-34851-z).
- [34] Mohsin Iqbal, Anasuya Lyons, Chiu Fan Bowen Lo, Nathanan Tantivasadakarn, Joan Dreiling, Cameron Foltz, Thomas M. Gatterman, Dan Gresh, Nathan Hewitt, Craig A. Holliman, Jacob Johansen, Brian Neyenhuis, Yohei Matsuoka, Michael Mills, Steven A. Moses, Peter Siegfried, Ashvin Vishwanath, Ruben Verresen, and Henrik Dreyer, “Qutrit toric code and parafermions in trapped ions,” *Nature Communications* **16** (2025), [10.1038/s41467-025-61391-z](https://doi.org/10.1038/s41467-025-61391-z).
- [35] M. S. Blok, V. V. Ramasesh, T. Schuster, K. O’Brien, J. M. Kreikebaum, D. Dahlen, A. Morvan, B. Yoshida, N. Y. Yao, and I. Siddiqi, “Quantum information scrambling on a superconducting qutrit processor,” *Phys. Rev. X* **11**, 021010 (2021).
- [36] A. Morvan, V. V. Ramasesh, M. S. Blok, J. M. Kreikebaum, K. O’Brien, L. Chen, B. K. Mitchell, R. K. Naik, D. I. Santiago, and I. Siddiqi, “Qutrit randomized benchmarking,” *Phys. Rev. Lett.* **126**, 210504 (2021).
- [37] Kai Luo, Wenhui Huang, Ziyu Tao, Libo Zhang, Yuxuan Zhou, Ji Chu, Wuxin Liu, Biying Wang, Jiangyu Cui, Song Liu, Fei Yan, Man-Hong Yung, Yuanzhen Chen, Tongxing Yan, and Dapeng Yu, “Experimental realization of two qutrits gate with tunable coupling in superconducting circuits,” *Physical Review Letters* **130** (2023), [10.1103/physrevlett.130.030603](https://doi.org/10.1103/physrevlett.130.030603).
- [38] Alba Cervera-Lierta, Mario Krenn, Alán Aspuru-Guzik, and Alexey Galda, “Experimental high-dimensional greenberger-horne-zeilinger entanglement with superconducting transmon qutrits,” *Phys. Rev. Appl.* **17**, 024062 (2022).
- [39] Xiao-Min Hu, Cen-Xiao Huang, Nicola d’Alessandro, Gabriele Cobucci, Chao Zhang, Yu Guo, Yun-Feng Huang, Chuan-Feng Li, Guang-Can Guo, Xiaoqin Gao, Marcus Huber, Armin Tavakoli, and Bi-Heng Liu, “Observation of genuine high-dimensional multi-partite non-locality in entangled photon states,” *Nature Communications* **16** (2025), [10.1038/s41467-025-59717-y](https://doi.org/10.1038/s41467-025-59717-y).
- [40] Xiao-Min Hu, Wen-Bo Xing, Chao Zhang, Bi-Heng Liu, Matej Pivoluska, Marcus Huber, Yun-Feng Huang, Chuan-Feng Li, and Guang-Can Guo, “Experimental creation of multi-photon high-dimensional layered quantum states,” *npj Quantum Information* **6** (2020), [10.1038/s41534-020-00318-6](https://doi.org/10.1038/s41534-020-00318-6).
- [41] Pei Liu, Ruixia Wang, Jing-Ning Zhang, Yingshan Zhang, Xiaoxia Cai, Huikai Xu, Zhiyuan Li, Jiaxiu Han, Xuegang Li, Guangming Xue, Weiyang Liu, Li You, Yirong Jin, and Haifeng Yu, “Performing  $SU(d)$  operations and rudimentary algorithms in a superconducting transmon qudit for  $d = 3$  and  $d = 4$ ,” *Phys. Rev. X* **13**, 021028 (2023).
- [42] Daniel J. Spencer, Andrew Tanggara, Tobias Haug, Derek Khu, and Kishor Bharti, “Qudit low-density parity-check codes,” (2025), [arXiv:2510.06495 \[quant-ph\]](https://arxiv.org/abs/2510.06495).
- [43] Sergey Bravyi, Matthew B. Hastings, and Spyridon Michalakis, “Topological quantum order: Stability under local perturbations,” *Journal of Mathematical Physics* **51**, 093512 (2010).
- [44] Sergey Bravyi and Matthew B Hastings, “A short proof of stability of topological order under local perturbations,” *Communications in mathematical physics* **307**, 609–627 (2011).
- [45] Héctor Bombín, “Structure of 2d topological stabilizer codes,” *Communications in Mathematical Physics* **327**, 387–432 (2014).
- [46] Jeongwan Haah, “Commuting pauli hamiltonians as maps between free modules,” *Communications in Mathematical Physics* **324**, 351–399 (2013).
- [47] Jeongwan Haah, “Algebraic methods for quantum codes on lattices,” *Revista colombiana de matematicas* **50**, 299–349 (2016).
- [48] Jeongwan Haah, “Classification of translation invariant topological Pauli stabilizer codes for prime dimensional qudits on two-dimensional lattices,” *Journal of Mathematical Physics* **62**, 012201 (2021).
- [49] Yu-An Chen and Yijia Xu, “Equivalence between fermion-to-qubit mappings in two spatial dimensions,” *PRX Quantum* **4**, 010326 (2023).
- [50] Blazej Ruba and Bowen Yang, “Homological invariants of pauli stabilizer codes,” *Communications in Mathematical Physics* **405**, 126 (2024).
- [51] Blazej Ruba and Bowen Yang, “Witt groups and bulk-boundary correspondence for stabilizer states,” (2025), [arXiv:2509.10418 \[math-ph\]](https://arxiv.org/abs/2509.10418).
- [52] Robbert Dijkgraaf and Edward Witten, “Topological gauge theories and group cohomology,” *Communications in Mathematical Physics* **129**, 393–429 (1990).
- [53] Xiao-Gang Wen, “Topological order and edge structure of  $\nu=1/2$  quantum hall state,” *Phys. Rev. Lett.* **70**, 355–358 (1993).
- [54] Alexei Kitaev, “Anyons in an exactly solved model and beyond,” *Annals of Physics* **321**, 2–111 (2006), january Special Issue.
- [55] H. Bombin and M. A. Martin-Delgado, “Topological quantum distillation,” *Phys. Rev. Lett.* **97**, 180501 (2006).
- [56] Michael Levin and Xiao-Gang Wen, “Detecting topological order in a ground state wave function,” *Phys. Rev. Lett.* **96**, 110405 (2006).
- [57] Xie Chen, Zheng-Cheng Gu, and Xiao-Gang Wen, “Complete classification of one-dimensional gapped quantum phases in interacting spin systems,” *Phys. Rev. B* **84**, 235128 (2011).
- [58] Michael Levin and Zheng-Cheng Gu, “Braiding statistics approach to symmetry-protected topological phases,” *Phys. Rev. B* **86**, 115109 (2012).
- [59] Xie Chen, Zheng-Cheng Gu, Zheng-Xin Liu, and Xiao-Gang Wen, “Symmetry-protected topological orders in interacting bosonic systems,” *Science* **338**, 1604–1606 (2012).
- [60] Hong-Chen Jiang, Zhenghan Wang, and Leon Balents, “Identifying topological order by entanglement entropy,” *Nature Physics* **8**, 902–905 (2012).
- [61] L. Cincio and G. Vidal, “Characterizing topological order by studying the ground states on an infinite cylinder,” *Phys. Rev. Lett.* **110**, 067208 (2013).
- [62] Zheng-Cheng Gu and Michael Levin, “Effect of interactions on two-dimensional fermionic symmetry-protected topological phases with  $Z_2$  symmetry,” *Phys. Rev. B* **89**, 201113 (2014).
- [63] Zheng-Cheng Gu, Zhenghan Wang, and Xiao-Gang Wen, “Lattice model for fermionic toric code,” *Phys. Rev. B* **90**, 085140 (2014).

- [64] Chao-Ming Jian and Xiao-Liang Qi, “Layer construction of 3d topological states and string braiding statistics,” *Phys. Rev. X* **4**, 041043 (2014).
- [65] H. Bombin, “Gauge color codes: Optimal transversal gates and gauge fixing in topological stabilizer codes,” (2015), [arXiv:1311.0879 \[quant-ph\]](https://arxiv.org/abs/1311.0879).
- [66] Beni Yoshida, “Topological phases with generalized global symmetries,” *Phys. Rev. B* **93**, 155131 (2016).
- [67] Anton Kapustin and Ryan Thorngren, “Higher symmetry and gapped phases of gauge theories,” in *Algebra, Geometry, and Physics in the 21st Century: Kontsevich Festschrift*, edited by Denis Auroux, Ludmil Katzarkov, Tony Pantev, Yan Soibelman, and Yuri Tschinkel (Springer International Publishing, Cham, 2017) pp. 177–202.
- [68] Yu-An Chen, Anton Kapustin, and Djordje Radicevic, “Exact bosonization in two spatial dimensions and a new class of lattice gauge theories,” *Annals of Physics* **393**, 234–253 (2018).
- [69] Tian Lan, Liang Kong, and Xiao-Gang Wen, “Classification of  $(3+1)$ D bosonic topological orders: The case when pointlike excitations are all bosons,” *Phys. Rev. X* **8**, 021074 (2018).
- [70] Meng Cheng, Nathanan Tantivasadakarn, and Chenjie Wang, “Loop braiding statistics and interacting fermionic symmetry-protected topological phases in three dimensions,” *Phys. Rev. X* **8**, 011054 (2018).
- [71] AtMa P. O. Chan, Peng Ye, and Shinsei Ryu, “Braiding with borromean rings in  $(3+1)$ -dimensional space-time,” *Phys. Rev. Lett.* **121**, 061601 (2018).
- [72] Bo Han, Huajia Wang, and Peng Ye, “Generalized wenzee terms,” *Phys. Rev. B* **99**, 205120 (2019).
- [73] Qing-Rui Wang, Yang Qi, and Zheng-Cheng Gu, “Anomalous symmetry protected topological states in interacting fermion systems,” *Phys. Rev. Lett.* **123**, 207003 (2019).
- [74] Yu-An Chen and Anton Kapustin, “Bosonization in three spatial dimensions and a 2-form gauge theory,” *Phys. Rev. B* **100**, 245127 (2019).
- [75] Tian Lan and Xiao-Gang Wen, “Classification of  $3+1$ D bosonic topological orders (ii): The case when some pointlike excitations are fermions,” *Phys. Rev. X* **9**, 021005 (2019).
- [76] Yu-An Chen, “Exact bosonization in arbitrary dimensions,” *Phys. Rev. Res.* **2**, 033527 (2020).
- [77] Yu-An Chen, Tyler D. Ellison, and Nathanan Tantivasadakarn, “Disentangling supercohomology symmetry-protected topological phases in three spatial dimensions,” *Phys. Rev. Res.* **3**, 013056 (2021).
- [78] Maissam Barkeshli, Yu-An Chen, Po-Shen Hsin, and Naren Manjunath, “Classification of  $(2+1)$ d invertible fermionic topological phases with symmetry,” *Phys. Rev. B* **105**, 235143 (2022).
- [79] Theo Johnson-Freyd, “On the classification of topological orders,” *Communications in Mathematical Physics* **393**, 989–1033 (2022).
- [80] Tyler D. Ellison, Yu-An Chen, Arpit Dua, Wilbur Shirley, Nathanan Tantivasadakarn, and Dominic J. Williamson, “Pauli stabilizer models of twisted quantum doubles,” *PRX Quantum* **3**, 010353 (2022).
- [81] Yu-An Chen and Sri Tata, “Higher cup products on hypercubic lattices: Application to lattice models of topological phases,” *Journal of Mathematical Physics* **64**, 091902 (2023).
- [82] Yu-An Chen and Po-Shen Hsin, “Exactly solvable lattice Hamiltonians and gravitational anomalies,” *SciPost Phys.* **14**, 089 (2023).
- [83] Maissam Barkeshli, Yu-An Chen, Sheng-Jie Huang, Ryohei Kobayashi, Nathanan Tantivasadakarn, and Guanyu Zhu, “Codimension-2 defects and higher symmetries in  $(3+1)$ D topological phases,” *SciPost Phys.* **14**, 065 (2023).
- [84] Ryohei Kobayashi and Guanyu Zhu, “Cross-cap defects and fault-tolerant logical gates in the surface code and the honeycomb floquet code,” *PRX Quantum* **5**, 020360 (2024).
- [85] Maissam Barkeshli, Yu-An Chen, Po-Shen Hsin, and Ryohei Kobayashi, “Higher-group symmetry in finite gauge theory and stabilizer codes,” *SciPost Phys.* **16**, 089 (2024).
- [86] Maissam Barkeshli, Po-Shen Hsin, and Ryohei Kobayashi, “Higher-group symmetry of  $(3+1)$ D fermionic  $\mathbb{Z}_2$  gauge theory: Logical CCZ, CS, and T gates from higher symmetry,” *SciPost Phys.* **16**, 122 (2024).
- [87] Zijian Liang, Bowen Yang, Joseph T. Iosue, and Yu-An Chen, “Operator algebra and algorithmic construction of boundaries and defects in  $(2+1)$ d topological pauli stabilizer codes,” (2025), [arXiv:2410.11942 \[quant-ph\]](https://arxiv.org/abs/2410.11942).
- [88] Ryohei Kobayashi, Yuyang Li, Hanyu Xue, Po-Shen Hsin, and Yu-An Chen, “Generalized statistics on lattices,” *Phys. Rev. X* **16**, 011010 (2026).
- [89] Zijian Liang, Yijia Xu, Joseph T. Iosue, and Yu-An Chen, “Extracting topological orders of generalized pauli stabilizer codes in two dimensions,” *PRX Quantum* **5**, 030328 (2024).
- [90] Zijian Liang, Ke Liu, Hao Song, and Yu-An Chen, “Generalized toric codes on twisted tori for quantum error correction,” *PRX Quantum* **6**, 020357 (2025).
- [91] Leonid P. Pryadko, Vadim A. Shabashov, and Valerii K. Kozin, “Qdistrnd: A gap package for computing the distance of quantum error-correcting codes,” *Journal of Open Source Software* **7**, 4120 (2022).
- [92] Edward Witten, “Quantum field theory and the jones polynomial,” *Communications in Mathematical Physics* **121**, 351–399 (1989).
- [93] Xiao-Gang Wen, “Topological orders and edge excitations in fractional quantum hall states,” *Advances in Physics* **44**, 405–473 (1995), <https://doi.org/10.1080/00018739500101566>.
- [94] Haruki Watanabe, Meng Cheng, and Yohei Fuji, “Ground state degeneracy on torus in a family of zn toric code,” *Journal of Mathematical Physics* **64** (2023), 10.1063/5.0134010.
- [95] Keyang Chen, Yuanting Liu, Yiming Zhang, Zijian Liang, Yu-An Chen, Ke Liu, and Hao Song, “Anyon theory and topological frustration of high-efficiency quantum low-density parity-check codes,” *Phys. Rev. Lett.* **135**, 076603 (2025).
- [96] Bruno Buchberger, “Bruno buchberger’s phd thesis 1965: An algorithm for finding the basis elements of the residue class ring of a zero dimensional polynomial ideal,” *Journal of Symbolic Computation* **41**, 475–511 (2006).
- [97] Sergey Bravyi and Barbara Terhal, “A no-go theorem for a two-dimensional self-correcting quantum memory based on stabilizer codes,” *New Journal of Physics* **11**, 043029 (2009).
- [98] Sergey Bravyi, David Poulin, and Barbara Terhal, “Tradeoffs for reliable quantum information storage in

- 2d systems,” *Phys. Rev. Lett.* **104**, 050503 (2010).
- [99] Google Quantum AI and Collaborators, “Quantum supremacy using a programmable superconducting processor,” *Nature* **574**, 505–510 (2019).
- [100] Han-Sen Zhong, Hui Wang, Yu-Hao Deng, Ming-Cheng Chen, Li-Chao Peng, Yi-Han Luo, Jian Qin, Dian Wu, Xing Ding, Yi Hu, Peng Hu, Xiao-Yan Yang, Wei-Jun Zhang, Hao Li, Yuxuan Li, Xiao Jiang, Lin Gan, Guangwen Yang, Lixing You, Zhen Wang, Li Li, Nai-Le Liu, Chao-Yang Lu, and Jian-Wei Pan, “Quantum computational advantage using photons,” *Science* **370**, 1460–1463 (2020).
- [101] Sepehr Ebadi, Tout T. Wang, Harry Levine, Alexander Keesling, Giulia Semeghini, Ahmed Omran, Dolev Bluvstein, Rhine Samajdar, Hannes Pichler, Wen Wei Ho, Soonwon Choi, Subir Sachdev, Markus Greiner, Vladan Vuletić, and Mikhail D. Lukin, “Quantum phases of matter on a 256-atom programmable quantum simulator,” *Nature* **595**, 227–232 (2021).
- [102] Lars S. Madsen, Fabian Laudenbach, Mohsen Falamarzi, Askarani, Fabien Rortais, Trevor Vincent, Jacob F. F. Bulmer, Filippo M. Miatto, Leonhard Neuhaus, Lukas G. Helt, Matthew J. Collins, Adriana E. Lita, Thomas Gerrits, Sae Woo Nam, Varun D. Vaidya, Matteo Menotti, Ish Dhand, Zachary Vernon, Nicolás Quesada, and Jonathan Lavoie, “Quantum computational advantage with a programmable photonic processor,” *Nature* **606**, 75–81 (2022).
- [103] Sergey Bravyi, Oliver Dial, Jay M. Gambetta, Darío Gil, and Zaira Nazario, “The future of quantum computing with superconducting qubits,” *Journal of Applied Physics* **132**, 160902 (2022).
- [104] Tom Manovitz, Sophie H. Li, Sepehr Ebadi, Rhine Samajdar, Alexandra A. Geim, Simon J. Evered, Dolev Bluvstein, Hengyun Zhou, Nazli Ugur Koyluoglu, Johannes Feldmeier, Pavel E. Dolgirev, Nishad Maskara, Marcin Kalinowski, Subir Sachdev, David A. Huse, Markus Greiner, Vladan Vuletić, and Mikhail D. Lukin, “Quantum coarsening and collective dynamics on a programmable simulator,” *Nature* **638**, 86–92 (2025).
- [105] Alexey A. Kovalev and Leonid P. Pryadko, “Quantum kronecker sum-product low-density parity-check codes with finite rate,” *Phys. Rev. A* **88**, 012311 (2013).
- [106] Nikolas P. Breuckmann and Jens N. Eberhardt, “Balanced product quantum codes,” *IEEE Transactions on Information Theory* **67**, 6653–6674 (2021).
- [107] Pavel Panteleev and Gleb Kalachev, “Degenerate quantum ldpc codes with good finite length performance,” *Quantum* **5**, 585 (2021).
- [108] Ting-Chun Lin and Min-Hsiu Hsieh, “c3-locally testable codes from lossless expanders,” in *2022 IEEE International Symposium on Information Theory (ISIT)* (2022) pp. 1175–1180.
- [109] Anthony Leverrier and Gilles Zemor, “Quantum Tanner codes,” in *2022 IEEE 63rd Annual Symposium on Foundations of Computer Science (FOCS)* (IEEE Computer Society, Los Alamitos, CA, USA, 2022) pp. 872–883.
- [110] Pavel Panteleev and Gleb Kalachev, “Asymptotically good quantum and locally testable classical ldpc codes,” in *Proceedings of the 54th Annual ACM SIGACT Symposium on Theory of Computing, STOC 2022* (Association for Computing Machinery, New York, NY, USA, 2022) p. 375–388.
- [111] Irit Dinur, Min-Hsiu Hsieh, Ting-Chun Lin, and Thomas Vidick, “Good quantum ldpc codes with linear time decoders,” in *Proceedings of the 55th Annual ACM Symposium on Theory of Computing, STOC 2023* (Association for Computing Machinery, New York, NY, USA, 2023) p. 905–918.
- [112] Renyu Wang, Hsiang-Ku Lin, and Leonid P Pryadko, “Abelian and non-abelian quantum two-block codes,” in *2023 12th International Symposium on Topics in Coding (ISTC)* (IEEE, 2023) pp. 1–5.
- [113] Hsiang-Ku Lin and Leonid P. Pryadko, “Quantum two-block group algebra codes,” *Phys. Rev. A* **109**, 022407 (2024).
- [114] Adam Wills, Ting-Chun Lin, and Min-Hsiu Hsieh, “Local testability of distance-balanced quantum codes,” *npj Quantum Information* **10**, 120 (2024).
- [115] Adam Wills, Ting-Chun Lin, and Min-Hsiu Hsieh, “Tradeoff constructions for quantum locally testable codes,” *IEEE Transactions on Information Theory* **71**, 426–458 (2025).
- [116] Zijian Liang and Yu-An Chen, “Self-dual bivariate bicycle codes with transversal clifford gates,” (2026), arXiv:2510.05211 [quant-ph].

### Appendix A: $\mathbb{Z}_2$ bivariate bicycle codes

This appendix collects representative instances of  $\mathbb{Z}_2$  bivariate bicycle (BB) codes, compiled from Ref. [90]. We adopt the polynomial description used there: each code instance is specified by a pair of Laurent polynomials  $f(x, y)$  and  $g(x, y)$  with  $\mathbb{Z}_2$  coefficients, together with a choice of boundary identifications that render the translation lattice finite. The latter are encoded by two twisted boundary vectors  $\vec{a}_1, \vec{a}_2 \in \mathbb{Z}^2$ .

For each choice of  $(f, g; \vec{a}_1, \vec{a}_2)$ , one obtains a qubit LDPC stabilizer code with parameters  $[[n, k, d]]_2$ , where  $k$  is the number of logical qubits and  $d$  is the code distance of the underlying stabilizer code. Since our goal here is to provide concrete test cases spanning a range of performance, we select examples with progressively larger values of the figure of merit  $kd^2/n$ . This quantity is a convenient summary statistic that combines rate and distance for finite-size comparisons; it does not by itself determine performance under a specific decoder or circuit-level noise model, but it is useful for organizing representative instances.

Table V lists the resulting code parameters, the defining polynomials  $f(x, y)$  and  $g(x, y)$ , the boundary vectors  $\vec{a}_1, \vec{a}_2$ , and the corresponding  $kd^2/n$  values. These instances serve as representative benchmarks in the main text for comparing finite-size behavior across different code constructions.

$[[n, k, d]]$	$f(x, y)$	$g(x, y)$	$\vec{a}_1$	$\vec{a}_2$	$\frac{kd^2}{n}$
[[18, 4, 4]]	$1 + x + xy$	$1 + y + xy$	(0, 3)	(3, 0)	3.56
[[30, 4, 6]]	$1 + x + x^2$	$1 + y + x^2$	(0, 3)	(5, 1)	4.8
[[42, 6, 6]]	$1 + x + xy$	$1 + y + xy^{-1}$	(0, 7)	(3, 2)	5.14
[[48, 4, 8]]	$1 + x + x^2$	$1 + y + x^2$	(0, 3)	(8, 1)	5.33
[[56, 6, 8]]	$1 + x + y^{-2}$	$1 + y + x^{-2}$	(0, 7)	(4, 3)	6.86
[[72, 8, 8]]	$1 + x + x^{-1}y^3$	$1 + y + x^3y^{-1}$	(0, 12)	(3, 3)	7.11
[[84, 6, 10]]	$1 + x + x^{-2}$	$1 + y + x^{-2}y^2$	(0, 14)	(3, -6)	7.14
[[90, 8, 10]]	$1 + x + x^{-1}y^{-3}$	$1 + y + x^3y^{-1}$	(0, 15)	(3, -6)	8.89
[[120, 8, 12]]	$1 + x + x^{-2}y$	$1 + y + xy^2$	(0, 10)	(6, 4)	9.6
[[144, 12, 12]]	$1 + x + x^{-1}y^{-3}$	$1 + y + x^3y^{-1}$	(0, 12)	(6, 0)	12
[[210, 10, 16]]	$1 + x + x^{-3}y^2$	$1 + y + x^{-3}y^{-1}$	(0, 21)	(5, 10)	12.19
[[248, 10, 18]]	$1 + x + x^{-2}y$	$1 + y + x^{-3}y^{-2}$	(0, 62)	(2, 25)	13.06
[[254, 14, 16]]	$1 + x + x^{-1}y^{-3}$	$1 + y + y^{-6}$	(0, 127)	(1, 25)	14.11
[[310, 10, 22]]	$1 + x + x^3y^2$	$1 + y + x^{-4}y^4$	(0, 31)	(5, 11)	15.61
[[360, 12, 24]]	$1 + x + x^{-1}y^3$	$1 + y + x^3y^{-1}$	(0, 30)	(6, 6)	19.2

TABLE V.  $\mathbb{Z}_2$  qubit LDPC codes compiled from Ref. [90]. The table reports the code parameters  $[[n, k, d]]$ , the corresponding polynomials  $f(x, y)$  and  $g(x, y)$ , the twisted boundary vectors  $\vec{a}_1, \vec{a}_2$ , and the metric  $kd^2/n$ .